Maciej PAŃCZYK

COMPARISON OF DECAY FUNCTION AND MAPPED INFINITE BOUNDARY ELEMENTS USAGE IN OPTICAL MAMMOGRAPHY

ABSTRACT *Among the methods of finding approximate numerical solutions, Boundary Element Method is a valuable choice to analyze an infinite area. In such cases the so-called open boundary numerical model of the analyzed object is created. One of two types of infinite boundary elements can be used to receive results without accuracy losses and with significant reduction of the mesh size. Implementation of two main lines of infinite boundary elements development, its advantages and disadvantages will be discussed on the example of optical mammography screening examination for early detection of breast cancer.*

Keywords: *Boundary Element Method, Infinite Elements, Optical Tomography*

1. INTRODUCTION

There are two main lines of infinite boundary elements development: decay functions infinite elements and mapped infinite elements. The first type uses special decay functions in conjunction with ordinary boundary element

Maciej PAŃCZYK, D.Sc.
e-mail: maciejp@cs.pollub.pl

Politechnika Lubelska,
Wydział Elektrotechniki i Informatyki,
Instytut Informatyki

PROCEEDINGS OF ELECTROTECHNICAL INSTITUTE, Issue 260, 2012

interpolation functions [2, 3, 4, 9]. In that case field variable tends monotonically to its far field value while reaching the element boundary adjacent to the infinite surroundings. Consequently along finite element length, variable changes in the way that reflects the physics of the problem up to infinity. The second type transforms the element from finite to infinite domain. Field variable will reach its far value following geometrical coordinates which extends into infinity [4, 5, 6, 11]. Changing the basic interpolation functions interferes into Boundary Element Method (BEM) fundamental rules. The application of infinite elements in the open edge of the object also requires to use special quadratic boundary elements. This constitutes another complication for most mesh generators. On the other hand the process of infinite elements incorporation into BEM is quite logical and results in significant hardware requirements and calculation time reduction. All major aspects of the implementation of both infinite elements types into BEM will be presented on the example of optical mammography.

2. INFINITE BOUNDARY ELEMENTS THEORY

The basic idea of the decay function infinite boundary element construction is that the standard basis interpolation functions N_i are multiplied by so called decay functions D_i [2, 3, 4, 9]. Two types of decay functions will be considered: reciprocal and exponential. Reciprocal decay functions for the decay in positive direction of ξ are as follows ([4] in chapter 3):

$$D_i(\xi) = \left[(\xi_i - \xi_0)/(\xi - \xi_0)\right]^n \tag{1}$$

where i corresponds to the node number, (ξ_o, η_o) is some origin point. This point must be outside infinite element on the opposite side to the one which extends to infinity, n has to be greater than the highest power of ξ encountered in N_i . If the decay is in the positive ξ direction then $\xi_o < -1$.

Respectively $\eta_o < -1$ for the decay in the positive η direction. This avoids a singularity within the element. For second order eight node quadrilateral elements basis interpolation functions $n = 3$ was chosen. Decay function infinite basis interpolation functions becomes:

$$M_i(\xi,\eta) = N_i(\xi,\eta)\cdot\left[(\xi_i - \xi_0)/(\xi - \xi_0)\right]^3 \tag{2}$$

For the exponential decay function of the form:

$$D_i(\xi) = \exp\left[(\xi_i - \xi)/L\right] \tag{3}$$

where L[m] is a length which determines the severity of the decay, basis infinite interpolation functions are given by:

$$M_i(\xi,\eta) = N_i(\xi,\eta)\cdot \exp\left[(\xi_i - \xi)/L\right] \tag{4}$$

The basis interpolation function N_i for standard eight nodes quadrilateral isoparametric boundary elements are given by the following formulas (5):

$$\begin{aligned}
N_0(\xi,\eta) &= -(1-\xi)(1-\eta)(1+\xi+\eta)/4,\\
N_1(\xi,\eta) &= (1-\xi^2)(1-\eta)/2,\\
N_2(\xi,\eta) &= -(1+\xi)(1-\eta)(1-\xi+\eta)/4,\\
N_3(\xi,\eta) &= (1+\xi)(1-\eta^2)/2,\\
N_4(\xi,\eta) &= -(1+\xi)(1+\eta)(1-\xi-\eta)/4,\\
N_5(\xi,\eta) &= (1-\xi^2)(1+\eta)/2,\\
N_6(\xi,\eta) &= -(1-\xi)(1+\eta)(1+\xi-\eta)/4,\\
N_7(\xi,\eta) &= (1-\xi)(1-\eta^2)/2.
\end{aligned} \tag{5}$$

Decay function infinite elements based on 8 node, the second type, quadrilateral standard boundary elements are presented in figure 1. It is to notice that it consists of 8 nodes. The only important thing is to keep correct relation between decay function and node numbers which decides in which direction the element, exactly the element properties (geometry remains unchanged) extends into infinity.

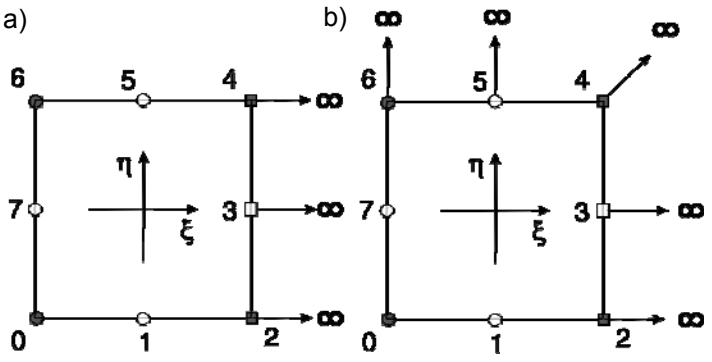

Fig. 1. Transformation of standard 8 node quadrilateral boundary element into decay type infinite element: a) in one positive ξ direction, b) in two positive ξ and η directions

Mapped infinite boundary elements based on 8 node, second type, quadrilateral standard boundary elements are presented in figure 2.

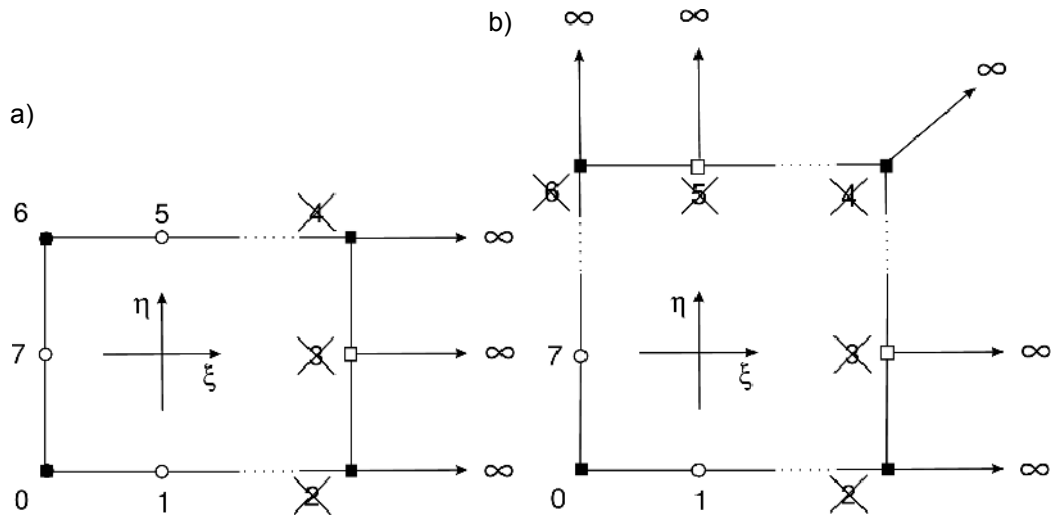

Fig. 2. Transformation of standard 8 node quadrilateral boundary element into mapped infinite element: a) in one positive ξ direction, b) in two positive ξ and η directions

It should be noticed that in such a case the element will consist only of 5 nodes. Nodes 2, 3, 4 tend to infinity and will not take part in the calculations.

Corresponding so called serendipity type basis interpolation functions $\hat{M}_i$ for mapped infinite elements are given by formula (6).

$$\begin{aligned}
\hat{M}_0 &= \frac{-1-\xi+\xi\eta+\eta^2}{1-\xi}, \\
\hat{M}_1 &= \frac{1+\xi}{1-\xi}\cdot\frac{1}{2}(1-\eta), \\
\hat{M}_5 &= \frac{1+\xi}{1-\xi}\cdot\frac{1}{2}(1+\eta), \\
\hat{M}_6 &= \frac{-1-\xi-\xi\eta+\eta^2}{1-\xi}, \\
\hat{M}_7 &= \frac{2}{1-\xi}\cdot(1-\eta^2).
\end{aligned} \tag{6}$$

Despite its name the procedure for deriving these functions is quite logical and clearly described by Zienkiewicz [12] (in chapter 7) or by Bettess [4]

(in chapter 4). The infinite basis interpolation functions $\hat{M}_i$ grow without limit as a coordinate approaches infinity, and are applied to the geometry. The ordinary basis interpolation functions N_i are applied to the field variables [7].

It is necessary to use these infinite basis interpolation functions to calculate Jacobian and regularization transformations. Analyzed area as well as corresponding integral equation will consists of both parts: finite and infinite surrounding of an open edge.

For debugging purposes, in case of ordinary basis interpolation functions one has to check if the sum of all basis interpolation functions is unity and if the sum of all their derivatives is zero. A simple test is to check if each function has unit value at its own node and zero at the other nodes. For decay type functions and for nodes remaining in the calculations in case of mapping functions that condition is also fulfilled. There is no exact analogy for the nodes which escape into infinity at mapped infinity elements. Further tests using Zienkiewicz type of mapped infinite elements [11] are devised by Bettess [4].

3. MODELS

Three simple theoretical models of human breast were investigated. For all models one placement of the light source was presented - located near the bottom of the hemisphere model. First model presented in fig.3 corresponds to the hemisphere with an additional cylindrical part in the bottom.

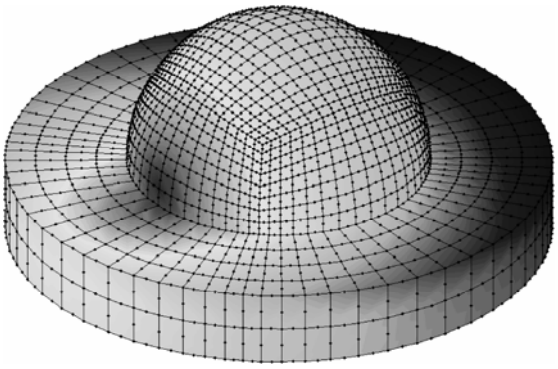

Fig. 3. Hemisphere breast model with an additional cylindrical part of chest on the bottom

Next two open boundary models use infinite boundary elements instead of additional cylindrical part. The area of interest is limited to hemisphere. Extra cylindrical part or infinite elements rings are necessary to add just to avoid possible errors which would occur in case of mesh truncation on the bottom

of the hemisphere. Standard boundary element model (fig. 3) was constructed from 1536 second order eight nodes quadrilateral boundary elements and 4610 nodes. Half of the elements covers the hemisphere.

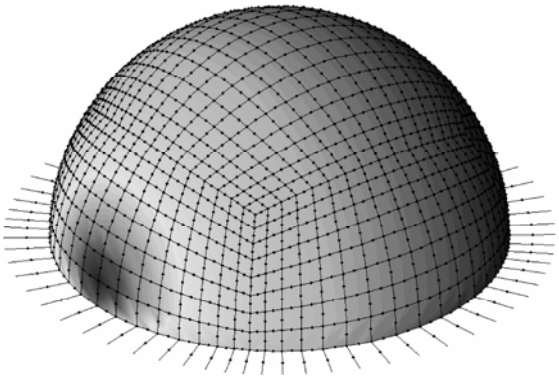

Fig. 4. Open boundary hemisphere breast model with mapped infinite boundary elements on the bottom

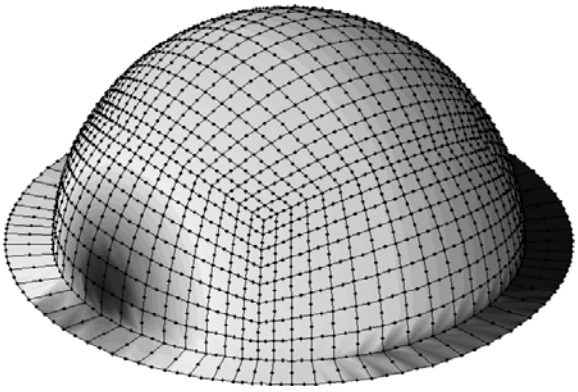

Fig. 5. Open boundary hemisphere breast model with decay function infinite boundary elements on the bottom

Open boundary model consists from 768 standard boundary elements and 64 infinite elements based on eight nodes second order quadrilateral boundary elements [5, 9]. The number of nodes was reduced to 2433 nodes in case of model with incorporated mapped infinite boundary elements and to 2561 nodes in case of decay function infinite element usage.

Governing equation for the problem is diffusion approximation of the transport equation [7] (Helmholtz (7) – assuming scattering and absorption are homogeneous). There are Robin boundary conditions (8) on surfaces [2, 8, 10]. In Diffusive Optical Tomography distribution of absorbing coefficient μ_a and reduced scattering coefficient μ_s' are investigated.

$$\nabla^2\Phi(\mathbf{r},\omega) - k^2\Phi(\mathbf{r},\omega) = -\frac{q_0(\mathbf{r},\omega)}{D}, \quad \forall \mathbf{r} \in \Omega/\Gamma, \tag{7}$$

where Φ stands for photon density, $k = \sqrt{\frac{\mu_a}{D} - j\frac{\omega}{cD}}$ complex wave number, $D = \left[3(\mu_a + \mu_S')\right]^{-1}[\mathrm{mm}^{-1}]$ diffusion coefficient, μ_S' is reduced scattering coefficient, μ_a is an absorbing coefficient, c speed of light in the medium, q_0 is a source of light (number of photons per volume unit emitted by concentrated light source located in position r with modulation frequency ω).

$$\Phi(\mathbf{r},\omega)+2\alpha D\frac{\partial\Phi(\mathbf{r},\omega)}{\partial n}=0,\quad \forall\mathbf{r}\in\Gamma. \tag{8}$$

with different coefficients for breast tissue and for skeletal muscles on the basis [2, 8, 10] imposed. In analysed example the following breast tissue properties were taken [2, 10]: $\mu_a = 0.025[\mathrm{mm}^{-1}], \mu_s' = 2[\mathrm{mm}^{-1}], \alpha = 1, f = 100\,\mathrm{MHz}$.

Relevant boundary integral equation for surfaces covered by standard and infinite elements can be written as:

$$\begin{aligned} &C(\mathbf{r})\Phi(\mathbf{r})+\int_{\Omega}\frac{\partial G(|\mathbf{r}-\mathbf{r}'|,\omega)}{\partial n}\Phi(\mathbf{r}')d\Omega+\\ &+\int_{\Omega_\infty}\frac{\partial G(|\mathbf{r}-\mathbf{r}'|,\omega)}{\partial n}\Phi(\mathbf{r}')d\Omega_\infty=\int_{\Omega}G(|\mathbf{r}-\mathbf{r}'|,\omega)\frac{\partial\Phi(\mathbf{r}')}{\partial n}d\Omega+\\ &+\int_{\Omega_\infty}G(|\mathbf{r}-\mathbf{r}'|,\omega)\frac{\partial\Phi(\mathbf{r}')}{\partial n}d\Omega_\infty-\sum_{S=0}^{n_S-1}Q_S G(|\mathbf{r_S}-\mathbf{r}|,\omega) \end{aligned} \tag{9}$$

where Q_S is the magnitude of the concentrated source ($q_0 = Q_S\delta(r_S)$) and n_S is a number of these sources, Φ stands for the photon density and G is the fundamental solution for the diffusion equation [2, 8, 10]. In 3D space for the diffusion equation the fundamental solution is [7]:

$$G(|\mathbf{r}-\mathbf{r}'|,\omega)=\frac{1}{4\pi|\mathbf{r}-\mathbf{r}'|}e^{-k|\mathbf{r}-\mathbf{r}'|}. \tag{10}$$

The normal derivative of the Green function in a direction n can be written:

$$\mathbf{n}\cdot\nabla G=\mathbf{n}\cdot\frac{\mathbf{r}-\mathbf{r}'}{|\mathbf{r}-\mathbf{r}'|}\left(\frac{-1}{4\pi|\mathbf{r}-\mathbf{r}'|^2}-\frac{k}{4\pi|\mathbf{r}-\mathbf{r}'|}\right)e^{-k|\mathbf{r}-\mathbf{r}'|}. \tag{11}$$

4. RESULTS

The values of $\partial\Phi/\partial n$ were already presented above in figures 3, 4 and 5. It is difficult to compare these color maps, especially that each model and its solution have its own range of values so the same color on all maps do not correspond to the same value. Taking that into account standard graphs were

used to compare the results precisely. The values of $\partial\Phi/\partial n$ module and phase of the light at nodes lying on hemisphere circumference cross-section for y = 0 are presented in figures 7 and 8 respectively. The values in nodes are presented in relation to angle Ψ (fig. 6).

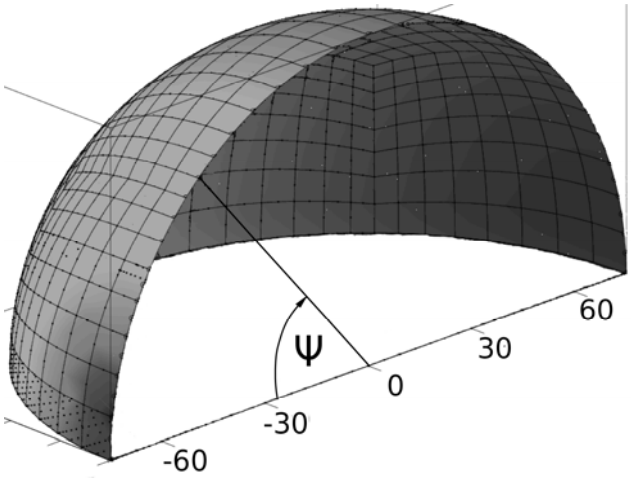

Fig. 6. Hemisphere circumference cross-section, $\partial\Phi/\partial n(\Psi)$ at y = 0

To estimate the solution differences, model with extended bottom part (fig. 3) was compared to these with infinite boundary elements implemented (fig. 4 and 5).

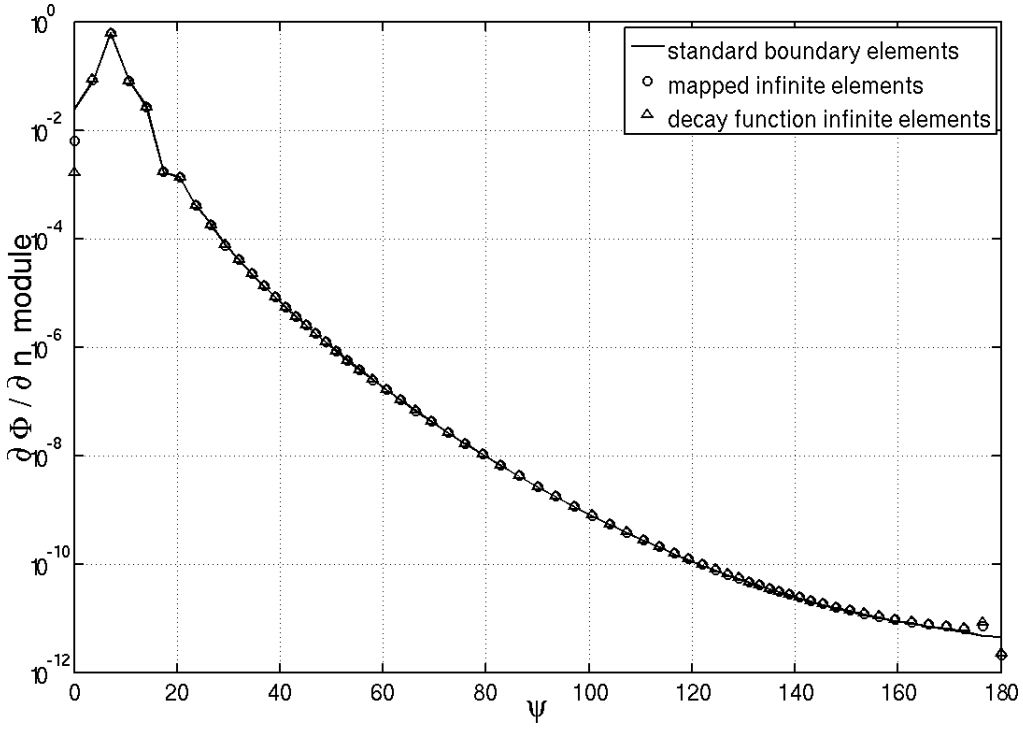

Fig. 7. Results comparison for $\partial\Phi/\partial n(\Psi)$ module and solution differences compared to hemisphere model

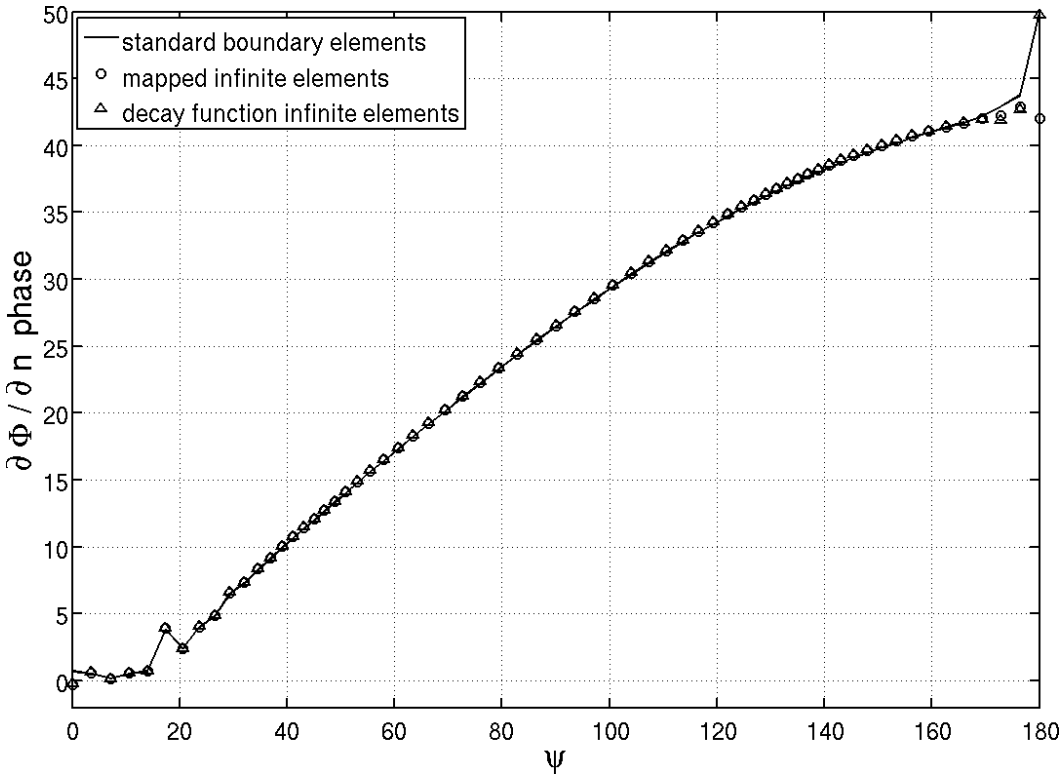

Fig. 8. Results comparison for $\partial\Phi/\partial n(\Psi)$ phase and solution differences compared to hemisphere model

Generally all results are similar. $\partial\Phi/\partial n(\Psi)$ values in nodes at about 30 degrees, like in figure 6 were collected in tables 1 (module) and 2 (phase). Except for single elements with common node for finite and infinite part of the model (for Ψ = 0 and Ψ = 180), maximum approximation differences for module is 10% (tab. 3) and for phase 3% (table 4).

TABLE 1
$\partial\Phi/\partial n(\Psi)$ module values for breast models built with standard, mapped infinite and decay function infinity boundary elements, at about 30 degrees (in the mesh nodes)

Ψ angle	0.0000	29.3577	60.6423	90.0000	119.3577	150.6423
standard	2.3680e-02	7.4592e-05	1.6034e-07	2.6032e-09	1.1834e-10	1.3232e-11
mapped	6.3776e-03	7.5688e-05	1.6340e-07	2.6669e-09	1.2206e-10	1.3887e-11
decay	1.6665e-03	7.6038e-05	1.6444e-07	2.6882e-09	1.2328e-10	1.4070e-11

TABLE 2
$\partial\Phi/\partial n(\Psi)$ phase values for breast models built with standard, mapped infinite and decay function infinity boundary elements at about 30 degrees (in the mesh nodes)

Ψ angle	0.0000	29.3577	60.6423	90.0000	119.3577	150.6423
standard	0.7204	6.5135	17.2974	26.4362	34.1462	39.8627
mapped	-0.2711	6.5912	17.3912	26.5452	34.2657	40.0082
decay	-0.2437	6.6123	17.4180	26.5756	34.3005	40.0443

TABLE 3
The $\partial\Phi/\partial n(\Psi)$ module differences in % between models with mapped infinite and with decay function infinity boundary elements compared to model built with pure standard elements, at about 30 degrees (in the mesh nodes)

Ψ angle	0.0000	29.3577	60.6423	90.0000	119.3577	150.6423
mapped	73.0680	1.4689	1.9122	2.4466	3.1417	4.9539
decay	92.9626	1.9385	2.5565	3.2617	4.1743	6.3317

TABLE 4
The $\partial\Phi/\partial n(\Psi)$ phase differences in % between models with mapped infinite and with decay function infinity boundary elements compared to model built with pure standard elements, at about 30 degrees (in the mesh nodes)

Ψ angle	0.0000	29.3577	60.6423	90.0000	119.3577	150.6423
mapped	137.6371	1.1928	0.5422	0.4124	0.3499	0.3648
decay	133.8253	1.5174	0.6969	0.5275	0.4519	0.4555

5. CONCLUSION

Both types of infinite boundary elements offer almost identical results, similar to these achieved by using standard model which contain only finite boundary elements. The role of the infinite elements is to receive the correct solution in the area of interest, so all additional parts like bottom cylinder in standard model (fig. 3) as well as ring build from infinite elements around the hemisphere (fig. 4 and 5) are neglected.

The advantage of using infinite elements is to avoid incorrect and unknown boundary conditions like on the surface between breast and chest in the breast models, to shorten the calculation time and keep the accuracy similar to standard solution (based on mesh extension, in our case mesh outside the hemisphere). All extended models were built from the same number of standard 8-node second order quadrilateral boundary elements. Mesh density on the additional surface related to cylindrical part of the model was lower then on the hemisphere surface. This is a typical practical solution, as the additional part represents the region outside the zone of interests.

Reducing the number of mesh elements almost to 50% is fundamental for inverse problem solution when the forward problem has to be calculated many times. Implementation of infinite boundary elements into boundary element method improves computational efficiency in case of the breast model almost 4 times and allows to avoid the problem of setting incorrect boundary

conditions. The process of incorporating infinite elements into BEM calculation scheme is quite logical and generally related to incorporation of new infinite basic approximation function and all further steps for its implications.

The main disadvantage for using infinite boundary elements is that not all mesh generators allow to create pure quadrilateral mesh or to distinguish separately areas covered by the most popular triangular elements and infinite part covered by quadrilateral 8 node elements. Moreover, the author doesn't know the generator which would allow to create 5 node infinite quadrilateral mapped elements.

Fortunately in optical mammography light sensors and sources are located in a special hemispherical or cone shape constant form so the effort related to manual creation of infinite element mesh which surrounds the area of interests has to be done only once.

There are two things to correct in the above models concerned to high differences on the values on single elements which have common nodes with infinite surroundings. First is to replace an acute angle on the border of finite and infinite parts with smooth transition. Second is to add some elements between these regions, so that infinite elements would not influence the area of investigated solution. Infinite elements are used just to achieve correct solution in the real area of interest. Their role is similar to mesh extension outside the region of interest used in standard method of treating open boundary objects. Therefore their nodes should not be a part of analyzed area. Actually implemented mesh and its corrections are presented in figure 9.

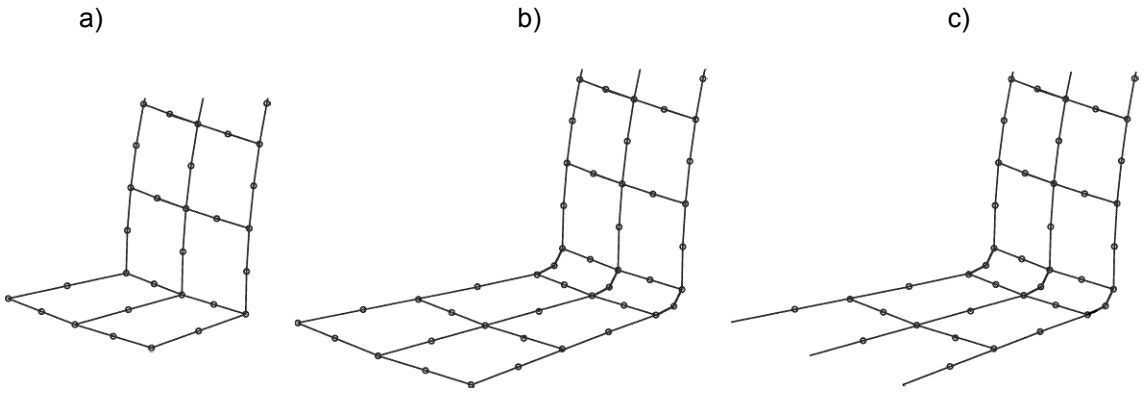

Fig. 9.
a) current mesh, b) proposed mesh modifications for decay functions infinite elements and for c) mapped infinite elements

Similar solution like presented in figure 9 for two-dimensional models with appropriative infinite elements solved successfully the last mentioned problem.

LITERATURE

1. Arridge S. R.: Optical tomography in medical imaging, Inverse Problems, vol. 15, No. 2 (1999), pp.R41{R93.
2. Beer G., Watson J. O. Infinite Boundary Elements, International Journal for Numerical Methods in Engineering, vol. 28 (1989), pp. 1233 – 1247.
3. Beer G., Watson J. O. and Swoboda G. Three-dimensional analysis of tunnels using infinite boundary elements, Computers and Geotechnics, vol. 3 (1987), pp. 37 – 58.
4. Bettess P. Infinite Elements, Penshaw Press, 1992.
5. Moser W., Duenser Ch. and Beer G. Mapped infinite elements for three-dimensional multiregion boundary element analysis, International Journal for Numerical Methods in Engineering, vol. 61 (2004), pp. 317 – 328.
6. Ross M. Modeling Methods for Silent Boundaries in Infinite Media, ASEN 5519- 006: Fluid-Structure Interaction Aerospace Engineering Sciences – University of Colorado at Boulder, 2004, http://www.colorado.edu/engineering/CAS/courses.d/FSI.d/FSI.projects.d/FSI.projects. Ross.silent.pdf
7. Sikora J. Boundary Element Method for Impedance and Optical Tomography, Oficyna Wydawnicza Politechniki Warszawskiej, Warsaw (2007).
8. Tarvainen T. Computational Methods for Light Transport in Optical Tomography, PhD Thesis, Department of Physics, University of Kuopio, (2006), http://physics.uku.fi/ ~vilhunen/phdthesis ttarvainen.pdf
9. Watson J. O. Advanced implementation of the boundary element method for two- and threedimensional elastostatics, Developments in Boundary Element Methods - 1 (Editors P.K. Banerjee and R. Butterfield), Elsevier Applied Science Publishers, vol. 61 (1979), pp. 31–63.
10. Zacharopoulos A., Arridge S. R., Dorn O., Kolehmainen V. and Sikora J. Three-dimensional reconstruction of shape and picewise constant region values for optical tomography using spherical harmonic parametrization and a boundary element method, Inverse Problems, vol. 22 (2006), pp.1-24.
11. Zienkiewicz C. O., Emson C. and Bettess P. A novel boundary infinite element, International Journal for Numerical Methods in Engineering, vol. 16 (1983), pp. 393 – 404.
12. Zienkiewicz C. O. The Finite Element Method, MCGraw-Hill, 4th edition, New York 1993.

Manuscript submitted 29.08.2012

PORÓWNANIE ELEMENTÓW BRZEGOWYCH NIESKOŃCZONYCH ODWZOROWANYCH I Z FUNKCJAMI ZANIKU W MAMMOGRAFII OPTYCZNEJ

Maciej PAŃCZYK

STRESZCZENIE *Spośród metod poszukiwania przybliżonego rozwiązania, do analizy obszarów nieograniczonych doskonale nadaje się metoda elementów brzegowych. W zagadnieniach takich*

tworzy się numeryczny model obiektu o tzw. otwartym brzegu. Można wówczas zastosować jeden z dwóch typów elementów brzegowych nieskończonych i bez pogorszenia dokładności wyników zmniejszyć rozmiar siatki elementów. Zalety i wady takiego rozwiązania jak również porównanie warunków implementacji obu gałęzi elementów nieskończonych w MEB zostaną omówione na przykładzie mammografii optycznej stosowanej do wczesnego przesiewowego wykrywania nowotworów piersi.

Słowa kluczowe: *Metoda elementów brzegowych, elementy brzegowe nieskończone, tomografia optyczna*

Maciej PAŃCZYK, PhD Eng. - graduated from the Faculty of Electrical Engineering, Lublin University of Technology. He worked in the Department of Fundamental Electrical Engineering, Lublin University of Technology, then in Information Technology Department in Bank BDK S.A and since 2004 at the Institute of Computer Science, Lublin University of Technology. His work focuses on the electromagnetic field and programming.